Dalton Transactions

Accepted Manuscript

ROYAL SOCIETY OF CHEMISTRY

www.rsc.org/dalton

Detection of host-guest interactions in clathrates of heterocyclic molecules adsorbed in a porous MOF with Cu_2 cluster nodes via vibration spectra and magnetic properties

Ping-Chun Guo, [a,b] Tian-Yu Chen, [a,b] Xiao-Ming Ren,*[a,b] Cheng Xiao, [a,b] and Wanqin Jin*[b]

[a] State Key Laboratory of Materials-Oriented Chemical Engineering, Nanjing University of Technology, Nanjing 210009, P.R. China.

[b] College of Science, Nanjing University of Technology, Nanjing 211816, P. R. China.

Fax: +86 25 58139481

Tel: +86 25 58139476

E-mail: xmren@njut.edu.cn (Ren); wqjin@njut.edu.cn (Jin)

Abstract

A three-dimensional NbO-type MOF with a formula $Cu_2(EBTC)(H_2O)_2 \cdot [G]$ (**1**) ($EBTC^{4-}$ = 1, 1′-ethynebenzene-3, 3′, 5, 5′-tetracarboxylate; G = guest molecules and represent DMF, DMSO and H_2O) was synthesized using solvothermal method. The enough cavity space in **1** can be used to encapsulate heterocyclic compounds benzopyrrole (C_8H_7N), benzofuran (C_8H_6O) and benzothiophene (C_8H_6S). The guest-free framework (**2**) was obtained by heating methanol-exchanged **1** at 130 °C under vacuum. The clathrates $[Cu_2(EBTC)(H_2O)_2 \cdot 1.6C_8H_7N]_\infty$ (**3**), $[Cu_2(EBTC)(H_2O)_2 \cdot 2.5C_8H_6O]_\infty$(**4**) and $[Cu_2(EBTC)(H_2O)_2 \cdot 2C_8H_6S]_\infty$ (**5**) were prepared by soaking **2** in C_8H_7N, C_8H_6O and C_8H_6S at 55 °C for 48 h, respectively. **1-5** showed quite similar PXRD patterns, indicating that they have the same framework structure. The IR and Raman spectra and the variable-temperature magnetic susceptibilities were comparatively studied for **1-5**; the results disclosed the existence of weakly intermolecular interactions between the parts of -C≡C- in the organic linkers and guest molecules, while almost complete absence of intermolecular interactions between the paddle-wheel-type dinuclear Cu_2 units and large guest molecules owing to steric hindrance. This study suggested the possibility of rather useful MOF materials in removal of organosulfur or organonitrogen compounds that are widely known contaminants in petroleum and fuels via the rational designed organic linkers.

Keywords: Cu-MOF, 1, 1’-ethynebenzene-3, 3’, 5, 5’-tetracarboxylate, guest-exchange, magnetic coupling, host-guest interaction

1. Introduction

Porous metal-organic frameworks (MOFs),[1-3] which are an emerging class of crystalline hybrid materials formed by the connection of metal centers or clusters and organic linkers. Highly ordered cavities and channels provided by MOFs are rationally designable and controllable, allowing guest molecules (typically gases and solvent molecules) to be absorbed and reside, moreover, the surface nature of the cavities or channels in a MOF can be modified via post-synthesis approach.[4, 5] These novel natures render the MOFs having the widespread applications in the fields of gas storage,[6] selective guest sorption[7-10] and separation[11] as well as sensors for detection of gases[12] or harmful organic compounds.[13-15] Meanwhile, many MOFs exhibit unique magnetic properties due to constitutive openshell transition metal ions, which has been attracting much attention[16-21] because of their potential applications in low density magnetic biomedicine and magnetic molecular sensors. It is interesting that some antiferromagnetic (AFM) Cu_2−SBUs constructed MOFs show ferromagnetic (FM) features,[16, 17, 22] which is identified Cu vacancies as the origin of localized spin states and local moments. The collective long-range ferromagnetism arises from the coupling between these localized spin states via delocalized π electrons in conjugated aromatic linkers and such a fascinating magnetic behavior is analogous to that observed in dilute magnetic semiconductors.[22] Recently, MOFs have been used to remove organosulfur or organonitrogen compounds from model fuels, which represent a type of alternative adsorbents that can be potentially used in the cost-effective production of low-sulfur or nitrogen fuels by selective adsorption.[23-34]

In the context of MOFs, the studies have also aroused much attention in host-guest chemistry. Given that the permanent pores or channels in the MOF material are generally filled by the guest molecules, such as lattice solvents or counterions, the host-guest interactions between the framework and the lattice solvent molecules/counterions as well as the disorder-to-order transformation of the polar guest molecules in the cavities or channels of MOFs provide a new promising platform for the creation of technologically important crystalline material. Over the

past decades, some fascinating phenomena have been observed in porous MOF magnets, such as guest-dependent spin crossover,[35-39] different magnetic behavior corresponding to reversible solvent-induced structural changes,[40] magnetic ordering sensitive to guest removal/exchange.[41] In addition, an intriguing ferroelectricity was observed in the MOF compound $[Mn_3(HCOO)_6]\cdot(C_2H_5OH)$, where the lattice ethanol molecules are loosely bound to the framework in the pores of the MOF and their orientation ordering results into the existence of net polarization and ferroelectricity;[42] a paraelectric-to-ferroelectric transition was triggered by the freeze of the disordered NH_4^+ counter cations in the pores of a MOF, where the H-bond donor NH_4^+ counter cations are incorporated into the negatively-charged metal formate framework of $[Zn(HCOO)_3]^-$;[43] and an anionic Fe–CN–K host framework with disordered imidazolium guest cations showed switchable dielectric behavior.[44] On the other hand, the host-guest interactions in MOF-based materials might be probed by comparatively investigating the change of features before and after the formation of clathrates.

In this study, we have synthesized a porous MOF compound with a formula $Cu_2(EBTC)(H_2O)_2\cdot[G]$ (**1**) ($EBTC^{4-}$ = 1, 1′-ethynebenzene-3, 3′, 5, 5′-tetracarboxylate; G = guest molecules and represent DMF, DMSO and H_2O), followed the published procedure,[45] using solvothermal method at 65 °C, further prepared the clathrates of benzothiophene, benzopyrrole and benzofuran in this porous framework via guest-exchange approach, such nitrogen and sulfur compounds in fuel oils as environmental pollutants are a major concern due to their exhaust gases containing SOx, NO_y, which not only contribute to acid rain but are also harmful to human health. We also investigated the thermal stability, and host-guest interactions via vibration spectra and magnetic properties for these compounds.

2. Experimental

2.1. Materials and measurements

All reagents (benzothiophene, benzopyrrole and benzofuran and so on) and solvents (methanol, DMF and DMSO) were obtained from chemical suppliers and used without further purification. 1, 1´-ethynebenzene-3, 3´, 5, 5´-tetracarboxylic acid

(H_4EBTC) was prepared following the published procedure.[46]

Power X-ray diffraction (PXRD) data were collected on a Bruker D8 diffractometer with Cu Kα radiation (λ = 1.5418 Å). Thermogravimetric (TG) experiments under a nitrogen atmosphere were performed with a STA449 F3 thermogravimetric analyzer from 30 to 600 °C at a warming rate of 10 °C/min and the polycrystalline samples were placed in an aluminum crucible. Fourier transform infrared (FT-IR) spectra were recorded on an IF66V FT-IR (4000–400 cm^{-1}) spectrophotometer with KBr disc. Far-infrared spectra were recorded at a resolution of 4 cm^{-1} on NICOLET 870 SX FT-IR (600–100 cm^{-1}) spectrophotometer. The samples were diluted in paraffin. Raman spectra were recorded by using a Renishaw Raman Microscope spectrometer. An Ar^+ laser emitting at 514 nm was used in which its output power was limited to 5% in order to avoid sample decomposition. Magnetic susceptibility data for polycrystalline samples were measured over a temperature range of 1.8–400 K using a Quantum Design MPMS-5S superconducting quantum interference device (SQUID) magnetometer; no correction was made for the diamagnetic susceptibility of the atomic cores.

2.2. Syntheses of samples

$[Cu_2(EBTC)(H_2O)_2 \cdot G]_\infty$ (**1**) was prepared following the published procedure.[45] The sample **1** was repeatedly exchanged by methanol for five times and then heated at 130 °C under vacuum overnight to give the guest-free sample of $[Cu_2(EBTC)]_\infty$ (**2**). The clathrate samples of $[Cu_2(EBTC)(H_2O)_2 \cdot 1.6C_8H_7N]_\infty$ (**3**), $[Cu_2(EBTC)(H_2O)_2 \cdot 2.5C_8H_6O]_\infty$ (**4**) and $[Cu_2(EBTC)(H_2O)_2 \cdot 2C_8H_6S]_\infty$ (**5**) were prepared by soaking **2** in C_8H_7N, C_8H_6O and C_8H_6S at 55 °C for 48 h and then washing with CH_2Cl_2 for three times, respectively.

3. Results and discussion

3.1 PXRD and TG analysis

MOF **1** crystallizes in the rhombohedral space group R-3m. As shown in Figure 1, the framework in **1** is comprised of paddle-wheel-type dinuclear Cu_2 units which are

connected through $EBTC^{4-}$ ligands to form a three-dimensional (3-D) NbO-type crystal structure and possesses two types of nanometer-sized cavities; the small cavity has ca. 8.5 Å in diameter and the larger one shows irregular elongated cavity with a dimensional of about 8.5×21.5 Å. The heavily disordered H_2O, DMF and DMSO guest molecules occupy in two types of cavities of **1**.[45] Notably, the cavities in **1** are sufficiently large to allow the heterocyclic molecules, such as benzopyrrole, benzofuran and benzothiophene, being encapsulated.

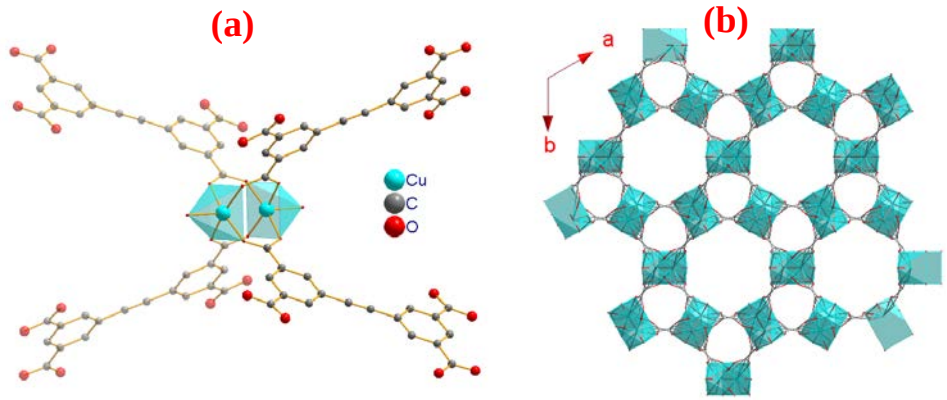

Figure 1 (a) Paddle-wheel-type dinuclear Cu_2 unit and the square pyramid coordination environment of Cu^{2+} ions, which basal plane is comprised from four oxygen atoms from carboxylate groups and the axial site is occupied by H_2O (b) 3-D NbO-type crystal structure with two types of nanometer-sized cavities in MOF **1**. [45]

The PXRD patterns of **1**–**5** are shown in Figure 2a. It is worth noting that the positions of the main diffraction peaks in PXRD profiles of **2**–**5** are in good accordance with those in **1**, implying that the host framework is unchanged after guest-exchange.

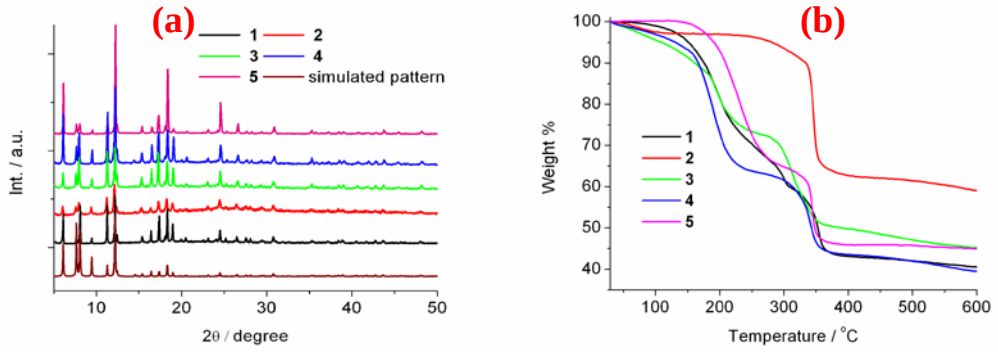

Figure 2 (a) Powder XRD patterns and (b) TG plots of **1**–**5**.

TG analyses were performed for **1**–**5** on crystalline samples between 30 and 600 °C at a warming rate of 10 °C/min under a nitrogen atmosphere, and the corresponding plots are shown in Figure 2b. For **1**, a series of consecutive weight loss of 40.2% occurs between 50 and 310 °C which corresponds to the removal of the guest molecules (DMF, DMSO and H_2O) and the coordinated H_2O molecules, and then the gradual collapse of the framework was observed above ca. 310 °C. For the guest-free **2**, the 3% H_2O molecules adsorbed during the test was lost up to 100 °C, and the pyrolysis procedure of the framework begins above 250 °C. The weight loss of **3**–**5** proceeds in two obvious steps. The first one corresponds to the release of the organic adsorbents and this procedure starts at ambient temperature for **3** and **4**. Interestingly, no weight loss was observed before 140 °C for **5**, suggesting that the C_8H_6S molecules bind to the host framework stronger than C_8H_7N and C_8H_6O molecules. The second weight loss process, which occurs above 300 °C, is due to the decomposition of the metal-organic-frameworks. Notably, **5** showed higher decomposition temperature of the framework than **3** **a**nd **4**. On the basis of TG analysis, the adsorbent molecules per $[Cu_2(EBTC)(H_2O)_2]$ formula unit were estimated to be ca. 1.6 for **3**, ca. 2.5 for **4** and ca. 2.0 for **5**, respectively.

3.2 IR and Raman spectra

The IR spectra in 4000–400 cm^{-1}, Far-IR spectra in 600–100 cm^{-1} and Raman spectra in 3000–50 cm^{-1} (using the λ = 514 nm laser) were performed for **1**–**5**. It is clear difference between Raman spectra of **1** and **2** and those of the clathrates **3**–**5**, especially **3** and **4**, which show weak Raman signals owing to the existence of strong fluorescence[47] excited by 514 nm lasers (ref. Figure 3a). The selected regions of spectra are displayed in Figure 3a-3f and the characteristic vibration bands together with their assignments are summarized in Table 1.

As shown in Figure 3b, the ν(C≡C) mode of organic links is observed at 2222, 2218, 2220 and 2225 cm^{-1} in Raman spectra for **1**, **2**, **4** and **5**, respectively, but is absence in Raman spectrum of **3** which is caused by the intense photoluminescent emission of the benzopyrrole molecules inside cavities of MOF. The ν(C≡C) band in **1**,

4 and **5** shifts slight towards high wavenumber side by comparison of the guest-free framework **2**, indicating the existence of intermolecular interactions between guest molecules and –C≡C– groups in the framework. The band at 1602 cm^{-1} is observed in Raman spectra of **1**, **2**, **4** and **5**, which is attributed to the *ν*(C=C) mode of the phenyl ring in the organic links; this band is almost independent on the guest molecules, demonstrating the presence of quite weak interactions between the phenyl ring of $EBTC^{4-}$ ligands and guest molecules owing to the steric hindrance.

As displayed in Figure 3c, only **1** shows an intense absorption band at 1045 cm^{-1} in IR spectrum, and this band arises from the stretch vibration of S=O in DMSO molecule. The vibrational models concerning $Cu_2C_4O_8$ copper oxide clusters appear in the low-frequency region (600–170 cm^{-1} range),[49,51] and a band appears around 505 cm^{-1} in Raman spectrum of guest-free compound **2** while shifts to around 487 cm^{-1} in Raman spectra of **1** and **5**. This distinction is probably related to the difference of coordination environment of Cu centers between guest-free **2** and others, or chemical pressure. However, the exact reason is unclear at present stage. In addition, The ν(Cu-O) and ν(Cu-Cu) bands are observed around 296 and 170 cm^{-1}, [51] respectively.

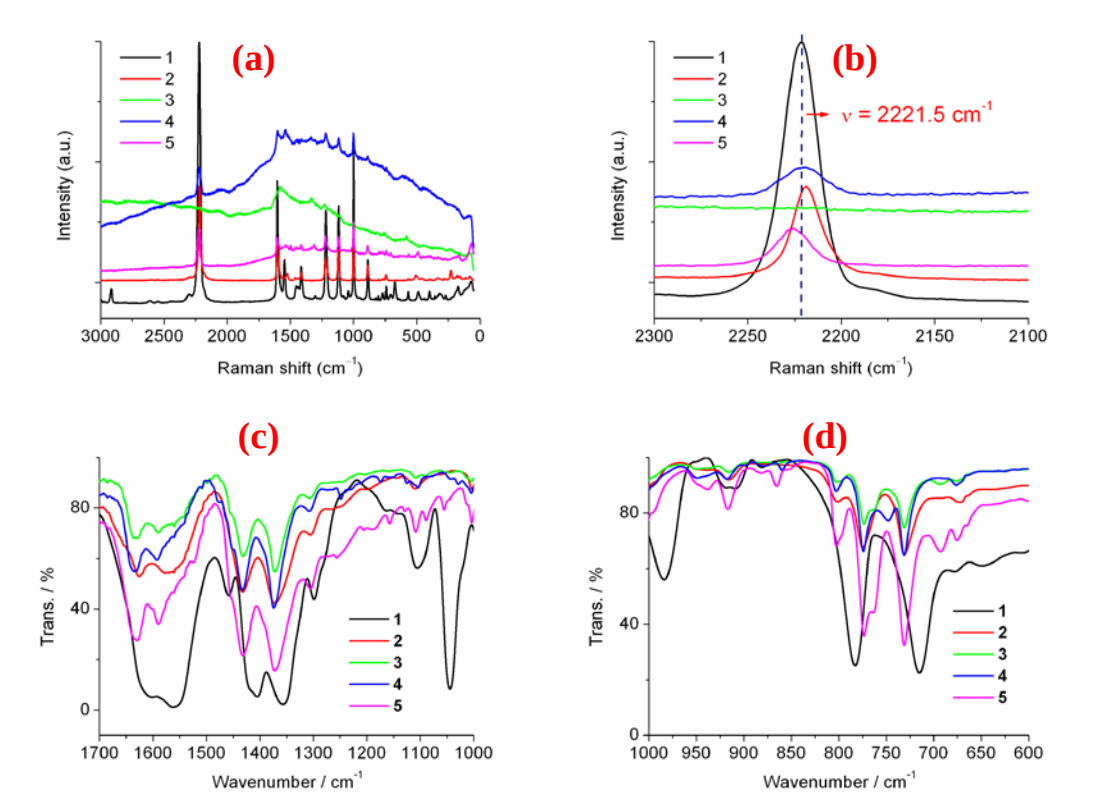

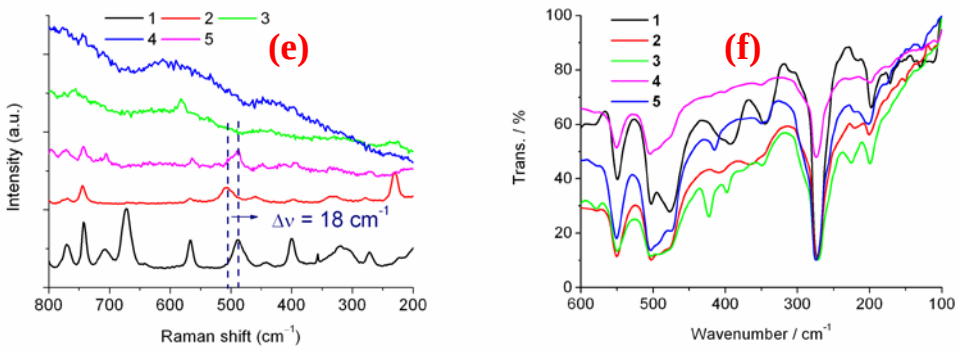

Figure 3 IR and Raman spectra of **1**–**5** in the region of (a) 3000–50 cm^{-1} (b) 2300–2150 cm^{-1} (c) 1700–1000 cm^{-1} (d) 1000–600 cm^{-1} (e) 800–200 cm^{-1} and 600–100 cm^{-1}.

Table 1: The characteristic vibration bands (cm^{-1}) of IR and Raman and assignments for **1-5**

1	**2**	**3**	**4**	**5**	Assignments
2222(R)	2218(R)	–	2220(R)	2225(R)	ν(C≡C)
1630(IR)	1626(IR)	1630(IR)	1635(IR)	1630(IR)	δ (H_2O)[48]
1602(R)	1602(R)	–	1602(R)	1602(R)	ν(C=C) in
1000(R)	1000 (R)	–	1000(R)	1000(R)	phenyl ring[49,50]
1598(IR)	1567(IR)	1591(IR)	1592(IR)	1589(IR)	ν_{as}(–COO)[51]
1548(R)	1524(IR)	–	1544(R)	1541(R)	ν_{as}(–COO)[49]
1452(IR)	1457(R)	–	1450(R)	1461(R)	ν_{s}(–COO)[49]
1045(IR)	–	–	–	–	ν(S=O)
783(IR)	773(IR)	773(IR)	773(IR)	773(IR)	δ(C-H) in
715(IR)	731(IR)	731(IR)	731(IR)	731(IR)	phenyl ring
487(R)	505(R)	–	–	487(R)	$Cu_2C_4O_8$
320(R)	328(R)	–	–	–	cluster[51]
296 sh (IR)	296sh (IR)	296sh (IR)	296sh (IR)	296sh (IR)	ν(Cu-O)[51]
171(R)	175(R)	–	–	170(R)	ν(Cu-Cu)[51]

Notes: IR and R represent infrared and Raman bands.

3.3 Magnetic properties

The magnetic coupling nature within a dinuclear Cu_2 unit is sensitive to the subtle structural deformation of core and strongly dependent on the nature of counterions,[52,53] for example, Kahn et al. elegantly demonstrated that in a series of dinuclear Cu^{2+} μ-oxalate complexes it was possible to ‘‘tune’’ the singlet-triplet energy gap ($2J/k_B$) over a wide range ($0 < 2J/k_B < 400$ cm^{-1}) by keeping the

[Cu(μ-oxalate)Cu]$^{2+}$ core constant and varying only the nature of the amine ligands.[54] Isik and coworkers theoretically studied the magnetic coupling nature for a series of the dinuclear Cu^{2+} complexes with the [Cu(μ-Cl)$_2$Cu]$^{2+}$ core and revealed that the Cu^{2+} ions may interact with either ferromagnetically or antiferromagnetically depending on the bridging angle of the ligand.[55] These studies indicated that the magnetic measurement is available to be used as a probe to detect the structural deformation of dinuclear Cu_2 core. Thus, the variable-temperature magnetic susceptibilities in the 1.8-400 K range were further measured for **1-5**.

Figure 4a-4e show the temperature dependence of magnetic susceptibility for **1**–**5**, where χ_m represents the molar magnetic susceptibility of a sample with one Cu^{2+} ion per formula unit and the diamagnetism contributed from the atom core were not corrected. For the as-prepared sample of **1**, a broad maximum appears around 250 K and the χ_m value exponentially drops below 250 K, indicating the existence of strong antiferromagnetic coupling in **1**; a small amount of Curie-Weiss type magnetic susceptibility becomes visible in the low temperature region, which arises from the lattice defects.[56] On the basis of the crystal structure analysis, the paddle-wheel-type dinuclear Cu_2 units are connected through $EBTC^{4-}$ ligands in the framework of **1**, the magnetic coupling interaction between the neighboring Cu_2 units is weak owing to the existence of great Cu…Cu distance (> 9.6 Å), as a result, the magnetic exchange model of a dimer with two S = 1/2 spins was selected to analyze the variable-temperature magnetic behavior of **1**, and the corresponding molar magnetic susceptibility formula (Bleaney–Bowers equation) is given in the Eq. (1), which is deduced from the spin Hamiltonian $\mathbf{H} = -2J\mathbf{S}_1\mathbf{S}_2$,[57,58]

$$\chi_m(\mathrm{dim}\,er) = \frac{Ng^2\mu_B^2}{k_BT} \cdot \frac{1}{3+\exp(-2J/k_BT)} \qquad (1)$$

Where χ_m is molar magnetic susceptibility of the dimer with one Cu^{2+} ion per formula unit, g is Landé factor, J represents the magnetic coupling constant within a dimer and other symbols have normal meanings. To take into account the paramagnetic impurity and the diamagnetic contribution from the atom cores, the experimental molar

magnetic susceptibility can be expressed below,

$$\chi_m = (1-\rho)\chi_m(\mathrm{dimer}) + \rho\frac{C}{T-\theta} + \chi_o \qquad (2)$$

In Eq. (2), ρ represents the molar fraction of paramagnetic impurity, C and θ are respectively Curie and Weiss constants and χ_0 stands for the temperature-independent magnetic susceptibility. The experimental molar magnetic susceptibility data in 1.8–400 K were fitted to Eq. (2) to give g = 2.01, J/k_B = -213 K, C = 0.039 emu K mol^{-1}, θ = -0.73 K, $\chi_0 = -1.7\times10^{-4}$ emu mol^{-1} and ρ = 0.034 for **1**.

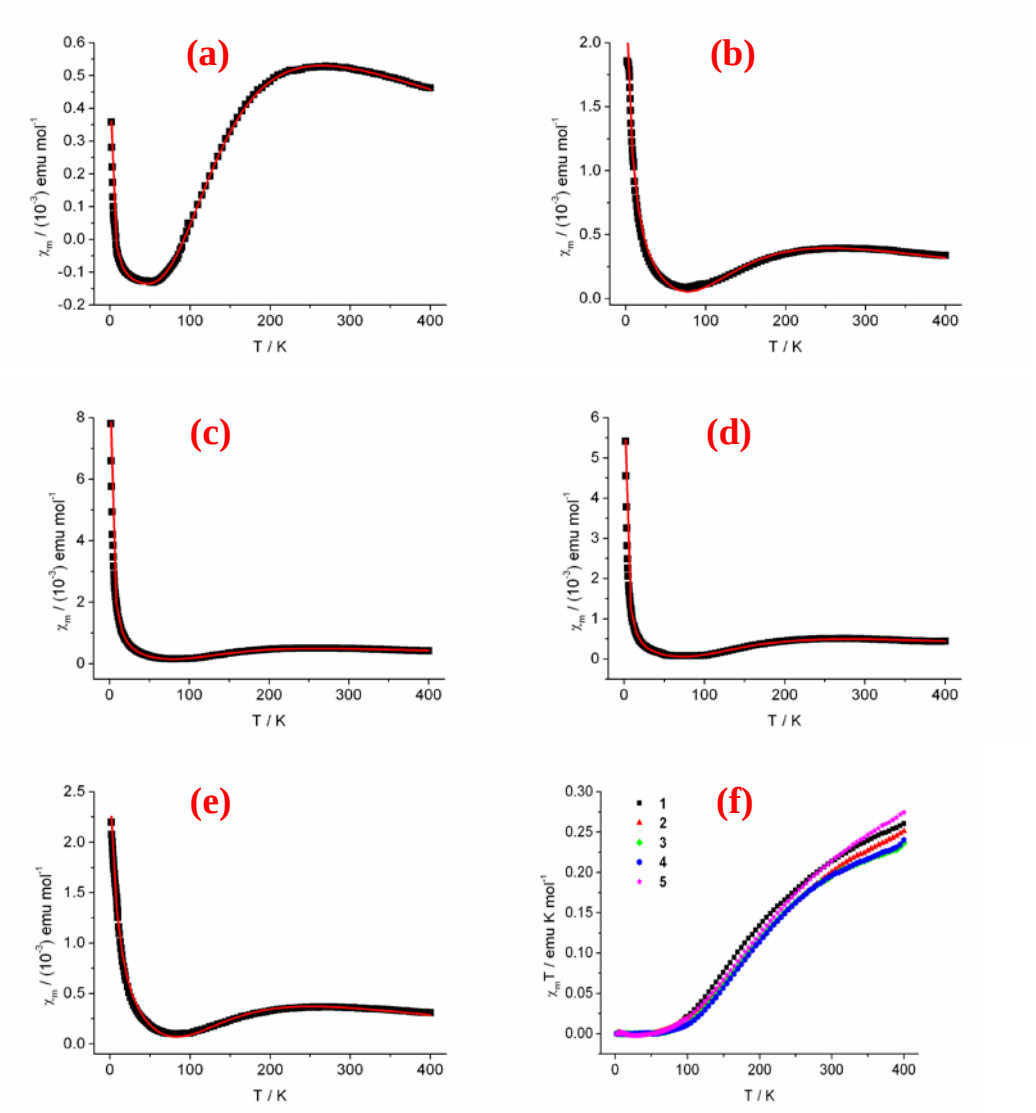

Figure 4 Temperature dependent magnetic susceptibility of (a) **1** (b) **2** (c) **3** (d) **4** (e) **5** and (f) χ_m(dimer)T-T plots for **1**–**5** where χ_m(dimer) represents the corrected paramagnetic susceptibility contributed from dinuclear Cu_2 unit.

As displayed in Figure 4b-4e, **2**–**5** show similar χ_m-T plots in 1.8–400 K range,

namely, a broad maximum occurs around 250 K and an enhanced low-temperature Curie-tail appears to indicate that there is a relatively large amount of paramagnetic impurity in **2**–**5** by comparison of **1**, this is due to that the guest removal and exchange in the preparation of **2**–**5** lead to the crystals broken, which produced a relatively large amount of lattice defects. The variable-temperature magnetic susceptibility data in 1.8–400 K range were fitted to Eq. (2) for **2**–**5**, and the parameters, g, J/k_B, C, θ, χ_0 and ρ obtained from the best fit are summarized in Table 2, from which we can found that the J/k_B values of **2**–**5** are close to that of **1**, suggesting that the guest molecules in the cavities of metal-organic framework do not significantly affect the magnetic coupling behavior within the paddle-wheel-type dinuclear Cu_2 unit and the presence of weakly intermolecular interactions between the guest molecules and the paddle-wheel-type dinuclear Cu_2 units. On the basis of the fits, the molar magnetic susceptibility contributed from the paddle-wheel-type dinuclear Cu_2 units, χ_m(dimer), was evaluated and the corresponding χ_m(dimer)T-T curves were plotted in Figure 4f for **1**–**5**, which are quite analogous to each other.

Table 2: The parameters obtained from variable-temperature magnetic susceptibility fits in 1.8–400 K range for **1**–**5**

	1	**2**	**3**	**4**	**5**
g	2.012	1.985	1.988	2.015	2.065
J/k_B / K	-213	-222	-228	-234	-226
C/emu·K·mol^{-1}	0.0393	0.163	0.150	0.118	0.192
θ / K	-0.73	-7.74	-0.60	-0.34	-10.34
χ_0 / emu·mol^{-1}	-1.7×10^{-4}	-2.6×10^{-4}	-1.4×10^{-4}	-1.3×10^{-4}	-1.7×10^{-4}
ρ	0.034	0.139	0.129	0.101	0.165
R^2	0.9996	0.9878	0.9999	0.9997	0.9954

4. Conclusion

In summary, we have prepared and characterized the clathrates $[Cu_2(EBTC)(H_2O)_2\cdot1.6C_8H_7N]_\infty$ (**3**), $[Cu_2(EBTC)(H_2O)_2\cdot2.5C_8H_6O]_\infty$ (**4**) and $[Cu_2(EBTC)(H_2O)_2\cdot2.0C_8H_6S]_\infty$ (**5**) using TG and PXRD techniques. The IR and Raman spectra and the variable-temperature magnetic susceptibility were comparatively studied for the as-prepared sample **1**, guest-free framework **2** and the

heterocyclic clathrates **3-5**, which gave the main results (1) the guest molecules in cavities of the framework does not affect the characteristic vibrational bands of the phenyl ring while results in the *ν*(C≡C) in the organic linker being small blue-shift and a vibrational model concerning $Cu_2C_4O_8$ copper oxide clusters being red-shift by comparison of guest-free framework; (2) the magnetic coupling nature within the paddle-wheel-type dinuclear Cu_2 unit is antiferromagnetic for **1-5** with similar magnetic exchange constants. These results disclosed the existence of weakly intermolecular interactions between the parts of -C≡C- in the organic linker and guest molecules, and almost complete absence of intermolecular interactions between the paddle-wheel-type dinuclear Cu_2 units and large guest molecules owing to steric hindrance. This study suggested the possibility of rather useful MOF materials in removal of organic sulfur or nitrogen compounds that are widely known contaminants in petroleum and fuels via the rational designed organic linkers.

Acknowledgements

This work was supported by National Nature Science Foundation of China (Grant no. 91122011, 21071080 and 21176115) and the Innovative Research Team Program by the Ministry of Education of China (No. IRT13070).

Notes and References

1. O. M. Yaghi, M. O'Keeffe, N. W. Ockwig, H. K. Chae, M. Eddaoudi and J. Kim, *Nature*, 2003, **423**, 705.
2. S. Kitagawa; R. Kitaura and S. Noro, *Angew. Chem., Int. Ed.*, 2004, **43**, 2334.
3. G. Férey, *Chem. Soc. Rev.*, 2008, **37**, 191.
4. K. L. Mulfort, O. K. Farha, C. L. Stern, A. A. Sarjeant and J. T. Hupp, *J. Am. Chem. Soc.*, 2009, **131**, 3866.
5. A. M. Shultz, A. A. Sarjeant, O. K. Farha, J. T. Hupp and S. T. Nguyen, *J. Am. Chem. Soc.*, 2011, **133**, 13252.
6. M. Dincă, A. F. Yu and J. R. Long, *J. Am. Chem. Soc.*, 2006, **128**, 8904.
7. O. M. Yaghi, G. M. Li and H. L. Li, *Nature*, 1995, **378**, 703.
8. D. N. Dybtsev, H. Chun, S. H. Yoon, D. Kim and K. Kim, *J. Am. Chem. Soc.*, 2004, **126**, 32.
9. G. Li, W. Yu and Y. Cui, *J. Am. Chem. Soc.*, 2008, **130**, 4582.
10. C. Zhu, G. Yuan, X. Chen, Z. Yang and Y. Cui, *J. Am. Chem. Soc.*, 2012, **134**, 8058.
11. J. R. Li, J. Sculley and H. C. Zhou, *Chem. Rev.*, 2012, **112**, 869.
12. N. Yanai, K. Kitayama, Y. Hijikata, H. Sato, R. Matsuda, Y. Kubota, M. Takata, M. Mizuno, T. Uemura and S. Kitagawa, *Nat. Mater.*, 2011, **10**, 787.
13. D. Britt, D. Tranchemontagne and O. M. Yaghi, *Proc. Natl. Acad. Sci. U. S. A.*, 2008, **105**, 11623.
14. Z. Z. Lu, R. Zhang, Y. Z. Li, Z. J. Guo and H. G. Zheng, *J. Am. Chem. Soc.*, 2011, **133**, 4172.
15. X. Q. Zou, J. M. Goupil, S. Thomas, F. Zhang, G. S. Zhu, V. Valtchev and S. Mintova, *J. Phys. Chem. C*, 2012, **116**, 16593.
16. S. S.-Y. Chui, S. M. F. Lo, J. P. H. Charmant, A. G. Orpen, I. D. Williams, *Science* 1999, **283**, 1184.
17. X. X. Zhang, S. S.-Y. Chui, I. D. Williams, *J. Appl. Phys.* 2000, **87**, 6007.

18. Y. Z. Zheng, M. L. Tong, W. Xue, W. X. Zhang, X. M. Chen, F. Grandjean, G. J. Long, *Angew. Chem., Int. Ed.* 2007, **46**, 6076.
19. B. Moulton, J. Lu, R. Hajndl, S. Hariharan, M. J. Zaworotko, *Angew. Chem., Int. Ed.* 2002, **41**, 2821.
20. S. C. Xiang, X. T. Wu, J. J. Zhang, R. B. Fu, S. M. Hu, X. D. Zhang, *J. Am. Chem. Soc.* 2005, **127**, 16352.
21. Y. Y. Sun, Y.-K. Kim, S. B. Zhang, *J. Am. Chem. Soc.* 2007, **129**, 12606.
22. L. Shen, S. W. Yang, S. Xiang, T. Liu, B. Zhao, M. F. Ng, J. Göettlicher, J. Yi, S. Li, L. Wang, J. Ding, B. Chen, S. H. Wei, Y. P. Feng, *J. Am. Chem. Soc.* 2012, **134**, 17286.
23. B. J. Liu, Y. B. Zhu, S. W. Liu and J. W. Mao, *J. Chem. Eng. Data*, 2012, **57**, 1326.
24. N. A. Khan, J. W. Jun, J. H. Jeong and S. H. Jhung, *Chem. Commun.*, 2011, **47**, 1306.
25. W. Dai, J. Hu, L. Zhou, S. Li, X. Hu and H. Huang, *Energy Fuels*, 2013, **27**, 816.
26. H. X. Zhang, H. L. Huang, C. X. Li, H. Meng, Y. Z. Lu, C. L. Zhong, D. H. Liu and Q. Y. Yang, *Ind. Eng. Chem. Res.*, 2012, **51**, 12449.
27. D. Peralta, G. Chaplais, A. Simon-Masseron, K. Barthelet and G. D. Pirngruber, *Energy Fuels*, 2012, **26**, 4953.
28. K. A. Cychosz, A. G. Wong-Foy and A. J. Matzger, *J. Am. Chem. Soc.*, 2008, **130**, 6938.
29. K. A. Cychosz, A. G. Wong-Foy and A. J. Matzger, *J. Am. Chem. Soc.*, 2009, **131**, 14538.
30. S. Achmann, G. Hagen, M. Hämmerle, I. Malkowsky, C. Kiener and R. Moos, *Chem. Eng. Technol.*, 2010, **33**, 275.
31. M. Maes, M. Trekels, M. Boulhout, S. Schouteden, F. Vermoortele, L. Alaerts, D. Heurtaux, Y. K. Seo,Y. K. Hwang, J. S. Chang, I. Beurroies, R. Denoyel, K. Temst, A. Vantomme, P. Horcajada, C. Serre and D. E. De Vos, *Angew. Chem., Int. Ed.*, 2011, **50**, 4210.

32. T. H. Park, K. A. Cychosz, A. G. Wong-Foy, A. Dailly and A. J. Matzger, *Chem. Commun.*, 2011, **47**, 1452.
33. N. A. Khan and S. H. Jhung, *Angew. Chem., Int. Ed.*, 2012, **51**, 1198.
34. B. Van de Voorde, A. S. Munn,N. Guillou,F. Millange,D. E. De Vos and R. I. Walton, *Phys. Chem. Chem. Phys.*, 2013, **15**, 8606.
35. Z. M. Wang, B. Zhang, H. Fujiwara, H. Kobayashi and M. Kurmoo, *Chem. Commun.*, 2004, 416.
36. G. J. Halder, C. J. Kepert, B. Moubaraki, K. S. Murray and J. D. Cashion, *Science*, 2002, **298**, 1762.
37. G. J. Halder, K. W. Chapman, S. M. Neville, B. Moubaraki, K. S. Murray, J. F. Létard and C. J. Kepert, *J. Am. Chem. Soc.*, 2008, **130**, 17552.
38. S. M. Neville, G. J. Halder, K. W. Chapman, M. B. Duriska, B. Moubaraki, K. S. Murray and C. J. Kepert, *J. Am. Chem. Soc.*, 2009, **131**, 12106.
39. P. D. Southon, L. Liu, E. A. Fellows, D. J. Price, G. J. Halder, K. W. Chapman, B. Moubaraki, K. S. Murray, J. F. Létard and C. J. Kepert, *J. Am. Chem. Soc.*, 2009, **131**, 10998.
40. K. Barthelet, J. Marrot, D. Riou and G. Férey, *Angew. Chem. Int. Ed.*, 2002, **41**, 281.
41. M. H. Zeng, X. L. Feng, W. X. Zhang and X. M. Chen, *Dalton Trans.*, 2006, 5294.
42. H. B. Cui, Z. M. Wang, K. Takahashi, Y. Okano, H. Kobayashi, A. Kobayashi and *J. Am. Chem. Soc.*, 2006, **128**, 15074.
43. G. C. Xu, X. M. Ma, L. Zhang, Z. M. Wang and S. Gao, *J. Am. Chem. Soc.*, 2010, **132**, 9588.
44. W. Zhang, Y. Cai, R. G. Xiong, H. Yoshikawa and K. Awaga, *Angew. Chem. Int. Ed.*, 2010, **49**, 6608.
45. Y. X. Hu, S. C. Xiang, W. W. Zhang, Z. X. Zhang, L. Wang, J. F. Bai and B. L. Chen, *Chem. Commun.*, 2009, 7551.

46. H. Zhou, H. Dang, J. H. Yi, A. Nanci, A. Rochefort and J. D. Wuest, *J. Am. Chem. Soc.*, 2007, **129**, 13774.
47. D. V. Martyshkin, R. C. Ahuja, A. Kudriavtsev, S. B. Mirov, *Rev. Sci. Instrum.* 2004, **75**, 630.
48. R. L. Frost, K. L. Erickson, J. Čejka, B. J. Reddy, *Spectrochim. Acta Part A: Mol. Biomol. Spectrosc.*, 2005, **61**, 2702.
49. C. Prestipino, L. Regli, J. G. Vitillo, F. Bonino, A. Damin, C. Lamberti, A. Zecchina, P. L. Solari, K. O. Kongshaug, S. Bordiga, *Chem. Mater.* 2006, **18**, 1337.
50. E. Biemmi, A. Darga, N. Stock, T. Bein, *Micropor. Mesopor. Mater.* 2008, **114**, 380.
51. K. Tan, N. Nijem, P. Canepa, Q. Gong, J. Li, T. Thonhauser, Y. J. Chabal, *Chem. Mater.*, 2012, **24**, 3153.
52. S. Youngme, P. Gunnasoot, N. Chaichit, C. Pakawatchai, *Trans. Met. Chem.* 2004, **29**, 840.
53. S. P. Foxon, O. Walter, R. Koch, H. Rupp, P. Müller, S. Schindler, *Eur. J. Inorg. Chem.* 2004, 344.
54. M. Julve, M. Verdaguer, O. Kahn, A. Gleizes, M. Philoche-Levisalles, *Inorg. Chem.* 1983, **22**, 368.
55. F. Isik, M. A. Sabaner, A. T. Akan, A. Bayri, *Indian J. Phys.* 2013, **87**, 241.
56. J. S. Pedersen, K. Carneiro, M. Almeida, *J. Phys. C: Solid State Phys.* 1987, **20**, 1781.
57. B. N. Figgis, R. L. Martin, *J. Chem. Soc.* 1956, 3837.
58. B. Bleaney, K. D. Bowers, *Proc. R. Soc. London, Ser. A* 1952, **214**, 415.

TOC

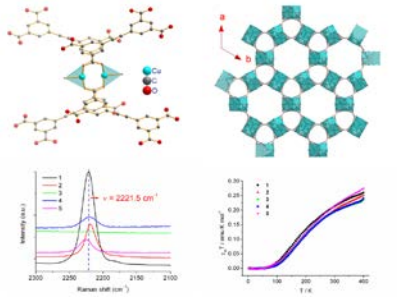

A 3-D MOF $Cu_2(EBTC)(H_2O)_2 \cdot [G]$ (**1**) shows enough cavity space; its guest-free framework (**2**) was used to encapsulate benzopyrrole (**3**), benzofuran (**4**) and benzothiophene (**5**) molecules. The host-guest interactions were studied via vibration spectra and magnetic susceptibility.